Journal of Power Sources 185 (2008) 1328–1333

Contents lists available at ScienceDirect

Journal of Power Sources

journal homepage: www.elsevier.com/locate/jpowsour

Analysis of self-sustaining recuperative solid oxide electrolysis systems

Sriram Gopalan[a,*], Mohsen Mosleh[a], Joseph J. Hartvigsen[b], Robert D. McConnell[c]

[a] Department of Mechanical Engineering, Howard University, 2300 6th Street, NW, Washington, DC 20059, United States
[b] Ceramatec Inc., 2425 South 900 West, Salt Lake City, UT 84119, United States
[c] Amonix Inc., 3425 Fujita Street, Torrance, CA 90505, United States

ARTICLE INFO

Article history:
Received 17 July 2008
Received in revised form 4 September 2008
Accepted 4 September 2008
Available online 19 September 2008

Keywords:
Solid oxide electrolysis cell (SOEC)
Thermoneutral voltage
Recuperative electrolysis
Hydrogen
Steam utilization

ABSTRACT

The generation of hydrogen through electrolysis possesses several advantages such as high efficiency, low pollution and decentralized fueling methods. In this paper, we show through modeling and simulation that the efficiency of hydrogen production can be further increased by operating the solid oxide electrolysis cell (SOEC) at the optimum combination of operating conditions. Specifically, the analysis of a recuperative SOEC that utilizes the thermal energy from the exhaust gases has revealed that operating the electrolysis cell above the thermoneutral voltage increased the efficiency of hydrogen production. We also found that the exit temperature of the gas streams depended on the operating voltage and steam utilization simultaneously. The effects of various operating parameters such as voltage, steam utilization, area specific resistance (ASR), the size of the heat exchangers, and the number of cells were analyzed in the system.

Published by Elsevier B.V.

1. Introduction

Hydrogen can be produced from natural gas, liquid fuels, biomass, water, biological systems and thermo-chemical cycles. Hydrogen is obtained from natural gas through a reforming process. Reforming is a catalytic reaction [1–4] at high temperatures and pressures that converts methane and steam into carbon dioxide and hydrogen (syngas). Hydrogen can also be produced using the partial oxidation of methane. This process, unlike the aforementioned reforming process, does not require the use of expensive catalysts. The disadvantages of these methods are the production of carbon dioxide as a by-product, which is not environmentally friendly, and the high cost of steam reforming plants. Hydrogen can also be produced through the gasification of coal [5]. This method involves converting coal into syngas, which is converted into hydrogen and carbon dioxide through a shift reaction. Although the gasification of coal is a well-established technology, the production of carbon dioxide and the environmental and sociological effects of coal mining and the resulting CO_2 emissions are serious disadvantages of hydrogen production by coal gasification.

The thermo-chemical cycle, such as a sulfur–iodine cycle, can be used to generate hydrogen with the aid of thermal energy. The reaction involves water reacting with sulfur dioxide and iodine to produce hydrogen iodide and sulfuric acid. At higher temperatures, hydrogen iodide disassociates into hydrogen and iodine [6]. This is a complex process because highly corrosive acids, such as sulfuric acid, are involved at temperatures as high as 1000 K, which makes it difficult for many materials to withstand. There are other challenges that need to be addressed such as the reactor design and the separation processes. The gasification or pyrolysis of biomass can also generate hydrogen. Biomass is readily available and a renewable source. However, biomass is a thinly distributed resource and unless small distributed processing facilities are employed the transportation costs may dominate. Pyrolysis or gasification of the biomass produces bio-oil, which is converted into syngas through a reforming process. This bio-oil is rich in several toxic materials and difficult to reform the compounds referred to BTX (benzene, toluene and xylene). The shift reaction of the syngas results in hydrogen. The disadvantages of this process are that 100 g of biomass yields only 8.6 g of hydrogen apart from the production of carbon dioxide [7].

1.1. Efficient generation of hydrogen by electrolysis of water

In contrast to production of hydrogen from fossil fuels and biomass, generation of hydrogen from water using solar energy is a clean process. A photosynthesis reaction can produce hydrogen by converting H^+ ions into hydrogen. The conversion is aided by green algae that provide an electron source and a catalyst for reaction. However, The efficiency of hydrogen generation using photosyn-

* Corresponding author. Tel.: +1 240 413 0346; fax: +1 703 440 9512.
E-mail address: gsriramgopalan@gmail.com (S. Gopalan).

0378-7753/$ – see front matter. Published by Elsevier B.V.
doi:10.1016/j.jpowsour.2008.09.027

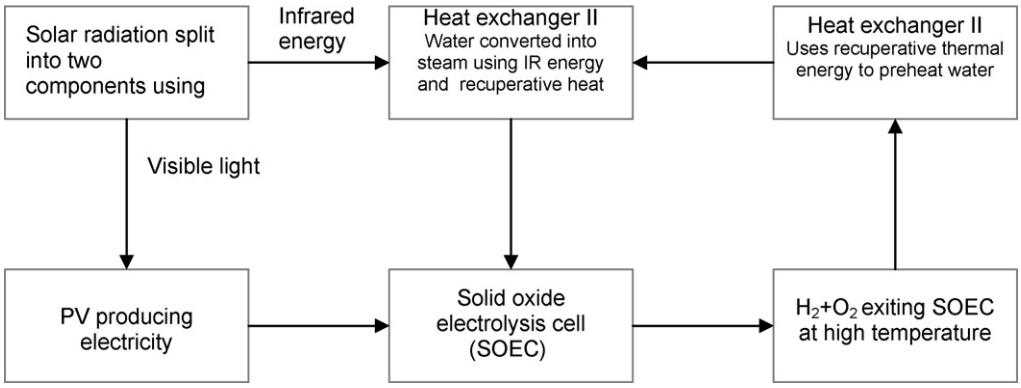

Fig. 1. Illustration of a recuperative, self-sustaining electrolysis system using solar renewable energy.

thesis is less than 1% [8,9]. The solar energy can be converted into the thermal energy, which can be employed for the direct thermal splitting of water into hydrogen and oxygen. The efficiency of solar energy conversion using this method ranges from 1% to 10% [9]. Researchers have proposed a photo-electrochemical process for water splitting using solar cells immersed in water [10,11]. A photovoltaic (PV) electrolysis method involves converting solar energy into electrical energy using a PV cell. The produced electrical energy will be used to operate an electrolysis cell to generate hydrogen. The efficiency of solar energy conversion to hydrogen production was found to be around 10–20% [9]. The theory for PV electrolysis process was developed and demonstrated experimentally [12–14]. The concentrator photovoltaic (CPV) method involves splitting concentrated solar energy spectrum using a dichroic filter into infrared and visible regions. The infrared (thermal energy) is used to generate heat and the visible light is used to provide electricity by means of photovoltaic cells to the electrolysis cell. The cost analysis for a concentrator photovoltaic system to produce hydrogen was previously reported [15]. It was found that hydrogen production through the CPV method was cheaper as the cost was \$3.18 kg^{-1} compared to the conventional PV electrolysis method which costs \$7.14 kg^{-1}. Two major reasons for the lower production cost were the PV cells with efficiencies over 40% and the use of solar infrared energy that is normally rejected as waste heat during the conventional concentrator PV operation.

Nuclear researchers have investigated hydrogen production by high temperature electrolysis through the heat and electricity generated from the nuclear reactor. A solid oxide fuel cell (SOFC) with reversed direction of current flow to split steam was utilized and referred to as solid oxide electrolysis cell (SOEC). Initial experimental and analytical results in this area appear promising [16–19].

In the absence of an associated high temperature heat source such as CPV or high temperature nuclear reactor, a SOEC still may be a more efficient means of hydrogen production than conventional electrolysis. Particularly, when paired with a CPV system during the day, the opportunity to continue operation at night without the benefit of the thermal input will be an important consideration in the overall process economics. For instance, if the SOEC system can be operated at night using only electricity from wind, hydro, or conventional nuclear power, the capital utilization factor and overall hydrogen production increases even thought the nighttime efficiency may go down. By careful thermal design it may be possible to operate the SOEC in a thermally self-sustaining mode while still obtaining higher efficiency that is possible with conventional water electrolysis. The theory of the use of waste heat from the solid oxide electrolysis cell has been proposed previously [20]. Since the system is complex, a theoretical model is needed to fully describe and better understand the system.

2. Analytical modeling

2.1. Self-sustaining recuperative electrolysis

We studied the recuperation of the exiting thermal energy from SOEC in order to further improve the efficiency of hydrogen production. The schematic of model of operation is shown in Fig. 1.

The system splits the solar radiation using a concentrator photovoltaic system and dichroic spectral splitter into infrared and visible spectrums of light. The visible light is transmitted to the photovoltaic cells where the solar energy is converted into electrical energy. The electrical energy is used by the solid oxide electrolysis cell to produce hydrogen and oxygen. The reflected infrared portion of the solar energy is used to convert the water to steam through heat exchanger I. The solid oxide electrolysis cell splits water into oxygen and hydrogen which exits at a very high temperature. The thermal energy from the SOEC is recuperated using heat exchanger II. This recuperated thermal energy can be used to convert water into steam in heat exchanger II.

2.2. Parametric modeling of recuperative SOEC

The exit temperature of the gas streams from the SOEC is calculated in three stages as shown in Fig. 2. The effect of operating voltage on the system was considered in the first stage. The operating voltage changed the composition of the inlet gas streams. This stage was operated in isothermal and adiabatic conditions. It is assumed that the temperature is maintained constant in this stage. It should be noted that as the area specific resistance (ASR) of the electrolyte is a function of temperature, a noticeable change in the system temperature might eventually affect the hydrogen production. This potential variation of temperature is not considered in this model for simplicity. Also, it is known that at the thermoneutral operating voltage or very close to it, there is either no or insignificant change in the system temperature. In the second stage, under adiabatic and non-isothermal conditions the effect of the operating voltage is evaluated. If the operating voltage is greater than the thermoneutral voltage, the system obtains more thermal energy and if the operating voltage is less than the thermoneutral value, there is a loss in the energy of the system. In the third stage, the effect of heat loss to the surroundings is taken into account. The loss in energy is a function of thickness of the insulation and the thermal conductivity of the insulator.

The mass flow rates of the inlet gas streams were calculated based on the operating voltage. The mole fraction of these gases was computed from the mass flow rates. The enthalpy of each gas stream was determined from the mole fraction of the gases at the

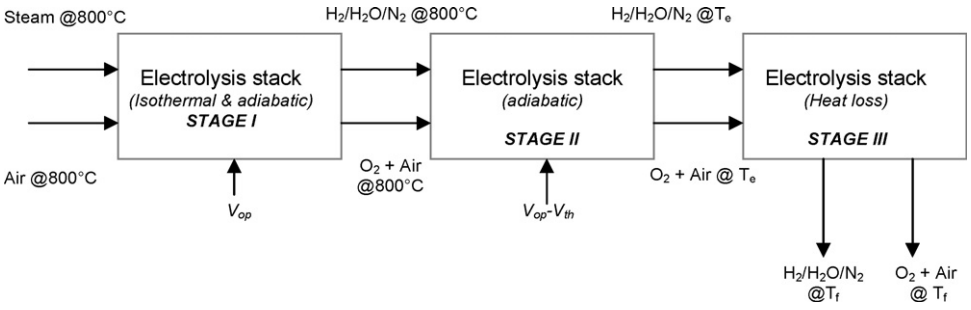

Fig. 2. Three stages of modeling of electrolysis.

desired temperature. The net enthalpy is given by

$$\Delta H_{\text{comp}} = H_{(H_2/H_2O/N_2)} + H_{(\text{Sweepair}+O_2)} - H_{(H_2O/H_2/N_2)} - H_{(\text{Sweepair})} \tag{1}$$

where ΔH_{comp} is the net change in enthalpy of the system, $H_{(H_2/H_2O/N_2)}$ is the enthalpy of the hydrogen stream exiting, $H_{(\text{Sweepair}+O_2)}$ is the enthalpy of the oxygen rich sweep air, $H_{(H_2O/H_2/N_2)}$ is the enthalpy of the inlet steam mixture and $H_{(\text{Sweepair})}$ is the enthalpy of the sweep air. The thermoneutral voltage is given by

$$V_{\text{tn}} = \frac{\Delta H_{\text{comp}}}{zF} \tag{2}$$

where V_{tn} is the thermoneutral voltage, z is the number of electrons transferred, F is the Faraday's constant.

If the electrolysis is operated at thermoneutral voltage, no extra heat is produced or consumed. The process takes place isothermally. But if the operating voltage is either above or below the thermoneutral voltage, the process can be either exothermic (heat produced) or endothermic (heat absorbed). The heat produced or absorbed is given by

$$Q_{\text{gen}} = (V_{\text{op}} - V_{\text{tn}})IN_{\text{cells}} \tag{3}$$

where Q_{gen} is the heat generated, V_{tn} is the thermoneutral voltage, V_{op} is the applied voltage, I is the current and N_{cells} is the number of electrolytic cells.

In the above system, the equation reduces to

$$(V_{\text{op}} - V_{\text{tn}})IN_{\text{cells}} = \Delta H_{\text{Stage II}} \tag{4}$$

$$\Delta H_{\text{StageII}} = \Delta H_{H_2/H_2O/N_2} + \Delta H_{(\text{Sweepair}+O_2)} \tag{5}$$

$$\Delta H_{H_2/H_2O/N_2} = \frac{dm(H_2O/H_2/N_2)}{dt} C_p(T_{\text{II}} - T_{\text{I}}) \tag{6}$$

$$\Delta H_{(\text{Sweepair}+O_2)} = \frac{dm_{(\text{Sweepair}+O_2)}}{dt} C_p(T_{\text{II}} - T_{\text{I}}) \tag{7}$$

where C_p is the specific heat at constant pressure, dm/dt is the mass flow rate of the respective gas streams.

Making the appropriate substitutions in the governing equation, it reduces to

$$T_{\text{II}} = T_{\text{I}} + \frac{(V_{\text{op}} - V_{\text{tn}})IN_{\text{cells}}}{(dm_{(H_2O/H_2/N_2)}/dt)C_{p(H_2O/H_2/N_2)} + (dm_{(\text{Sweepair}+O_2)}/dt)C_{p(\text{Sweepair}+O_2)}} \tag{8}$$

where T_{II} is the temperature at the end of stage II and T_{I} is the temperature at the end of stage I. Based on the insulation material and its thickness, there will be some heat loss. This heat loss given by the following expressions causes a drop in temperature at which the gases are exhausted:

$$Q_{\text{loss}} = kA\frac{T_{\text{II}} - T_0}{t} \tag{9}$$

where k is the thermal conductivity of the insulator, A is the insulation's cross-sectional area normal to the heat flux, t is the thickness of the insulator, T_0 is the temperature of the ambience. The final temperature at which the gases exit is given by

$$T_{\text{III}} = T_{\text{II}} - \frac{kA((T_{\text{II}} - T_0)/t)}{(dm_{(H_2O/H_2/N_2)}/dt)C_{p(H_2O/H_2/N_2)} + (dm_{(\text{Sweepair}+O_2)}/dt)C_{p(\text{Sweepair}+O_2)}} \tag{10}$$

where T_{III} is the temperature at the end of stage III.

2.3. Design of heat exchanger

The design of heat exchanger to recuperate heat from the gas streams leaving the solid oxide electrolysis cell is presented here. The heat is utilized for warming the fuel/sweep air entering the electrolysis cell. The governing equation for a heat exchanger design is

$$Q = U\,A\,LMTD \tag{11}$$

where Q is the Overall heat duty required, U is the overall heat transfer coefficient, and $LMTD$ is the Log Mean Temperature Difference. The log mean temperature difference of a heat exchanger with counter current flow can be given as

$$LMTD = \frac{(T_{\text{H\_IN}} - T_{\text{C\_OUT}}) - (T_{\text{H\_OUT}} - T_{\text{H\_IN}})}{LN((T_{\text{H\_IN}} - T_{\text{C\_OUT}})/(T_{\text{H\_OUT}} - T_{\text{H\_IN}}))} \tag{12}$$

where $T_{\text{H\_IN}}$ is the temperature at which the hot stream enters the heat exchanger (leaving the SOEC), $T_{\text{C\_OUT}}$ is the temperature at which the gas stream exits the heat exchanger (entering the SOEC), $T_{\text{H\_OUT}}$ is the temperature at which the hot stream exits the heat exchanger after cooling down, $T_{\text{H\_IN}}$ is the temperature at which main stream enters the heat exchanger. In the above equation $T_{\text{H\_IN}}$ is the temperature at which the gas exits the SOEC, which is determined, $T_{\text{C\_IN}}$ is the temperature at which gas streams enter which is usually room temperature. $T_{\text{C\_OUT}}$ is the required temperature at which the gas should enter the SOEC, which can be fixed at around 800–830 °C. So the only unknown quantity $T_{\text{H\_OUT}}$ can be determined from the energy balance of the in-streams and out-streams.

$$T_{\text{H\_OUT}} = T_{\text{H\_IN}} - \frac{\Delta H_{(H_2O/H_2/N_2)} + \Delta H_{(\text{Sweepair}+O_2)}}{(dm_{(H_2O/H_2/N_2)}/dt)C_{p(H_2O/H_2/N_2)} + (dm_{(\text{Sweepair}+O_2)}/dt)C_{p(\text{Sweepair}+O_2)}} \tag{13}$$

where ΔH is the change in the enthalpy of the respective streams that receives the recuperative heat. Since all the temperatures are known, $LMTD$ of the heat exchanger is calculated. Substituting $LMTD$ in the governing equation yields UA of the heat exchanger. The overall heat duty of the heat exchanger is a known quantity, which is given as

$$Q_{\text{net}} = Q_{\text{Air}} + Q_{\text{Fuel}} \tag{14}$$

where Q_{Fuel} is the heat duty required for the fuel stream and Q_{Air} is the heat duty required for the air stream.

In order to estimate the area of the heat exchanger, the overall heat transfer coefficient and the convective heat transfer coefficient of the gas streams are calculated as shown below:

$$h = \frac{Nu\,k}{D} \tag{15}$$

$$U_{air} = \frac{1}{(1/h_{hotair}) + (t/k) + (1/h_{coldair})} + \frac{1}{(1/h_{hot-H_2/H_2O/N_2}) + (t/k) + (1/h_{coldair})}$$
$$U_{H_2/H_2O/N_2} = \frac{1}{(1/h_{hotair}) + (t/k) + (1/h_{cold-H_2/H_2O/N_2})} + \frac{1}{(1/h_{hot-H_2/H_2O/N_2}) + (t/k) + (1/h_{cold-H_2/H_2O/N_2})} \tag{16}$$

where h is the convective heat transfer coefficient, Nu is the Nusselt number, k is the thermal conductivity of the channel, D is the characteristic length or the hydraulic diameter of the channel. Nusselt number is a dimensionless number that for laminar flow conditions depends only on channel cross-section geometry [21]. The thermal conductivity of gas mixtures in each channel was calculated as a function of temperature, pressure and the composition of the respective streams. After calculating the overall heat transfer coefficient the area A of the heat exchanger is calculated from UA. Then the number of plates is calculated from the dimensions of the flat plate.

2.4. Efficiency

Conventionally, the efficiency of electrolysis is given as the ratio of the lower heating value of the hydrogen produced to that of the product of the operating voltage and current [22]:

$$\eta_{electrolysis} = \frac{LHV}{V_{op} I} \tag{17}$$

Wherein our model apart from the electrical power applied, there are other sources of energy that are applied such as

1. Fan power to compensate for the pressure drop in the heat exchanger.
2. Thermal power to heat the gas streams, if required.

The pressure drop of the gas streams is a very important factor in the design of heat exchangers. Pressure drop is given as

$$\Delta P = \left(\frac{f\rho v^2}{2D}\right) L \tag{18}$$

where ΔP is the pressure drop, f is the friction factor, i is the density, v is the velocity of the gas streams, D is the hydraulic diameter, and L is the length of the channel through which the streams flow. The friction factor for laminar flow through narrow ducts can be obtained from the developed theories in the literature [23]. The fan power required to compensate for the pressure drop is found by

$$\text{FanPower} = \frac{\Delta P(dm/dt)}{\rho} \tag{19}$$

where dm/dt is the mass flow rate of the stream through the channel.

It has been proposed that gas streams entering the SOEC (rather than providing the heat through a furnace) will be heated through a heat exchanger. The source of heat for this heat exchanger will be the hot exhaust gases exiting SOEC. If the streams exiting the SOEC are not hot enough, then it has to be heated to the desired temperature before it entered the heat exchanger. The extra amount of heat that has to be supplied should be equal to

$$Q_{extra} = \frac{dm_{(H_2O/H_2/N_2)}}{dt} C_{p\_avg(H_2O/H_2/N_2)}(T_{desired} - T_{exit}) + \frac{dm_{(Sweepair+O_2)}}{dt} C_{p\_avg(Sweepair+O_2)}(T_{desired} - T_{exit})$$

The net efficiency of the model should be the ratio of the lower heating value of hydrogen produced to the sum of electrical power, fan power and the extra heating energy that is provided:

$$\eta_{actual} = \frac{\text{LowerHHV}}{(V_{op} I + Q_{extra} + \text{FanPower})} \tag{20}$$

3. Simulation and results

A computer code was generated with Visual Basic for simulation of the developed model at various combinations of the operating parameters. The voltages were varied from 1 to 2.5 V in steps of 0.1 V. Five different values of 22.8%, 45%, 60%, 75% and 90% for steam utilization were used. The parameters that were constant are stoich (sweep air flow relative to current), insulation thermal conductivity and thickness, SOEC area specific resistance, and the area of the electrolyte.

The variation of exit temperatures of the gas mixture as a function of steam utilization and operating voltage is given in Fig. 3. As the steam utilization value increased, the exit temperature of the gases decreased if the operating voltage was below the thermoneutral voltage. At the thermoneutral voltage, there was no change in the temperature irrespective of the change in the steam utilization value. Above the thermoneutral voltage, the exit temperature of the gas streams increased at higher steam utilization value. A mathematical explanation can be offered for the above mentioned behavior. Applying the energy balance to the equation it follows that:

$$\dot{Q} = (V_{op} - V_{tn})I$$
$$\dot{H} = \dot{N}(C_p dT) \tag{21}$$

Substituting for the current in the equation in terms of steam utilization:

$$I = (\dot{N} z F) S U \tag{22}$$

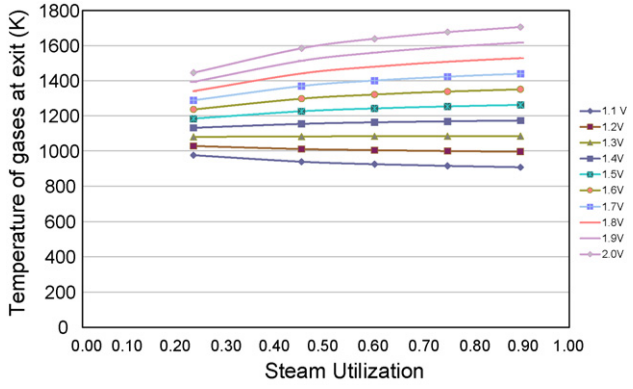

Fig. 3. Temperature of gases at exit versus steam utilization for various operating voltages.

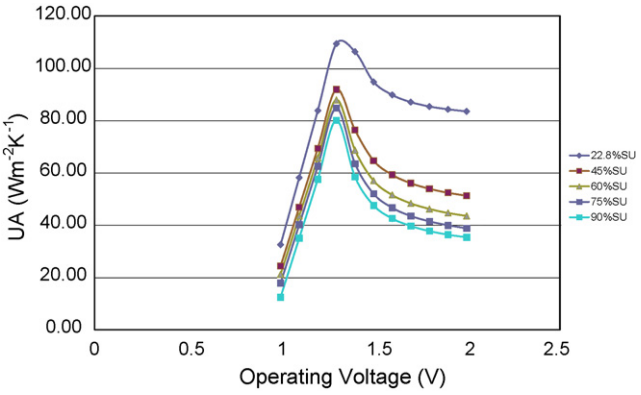

Fig. 4. UA of the heat exchanger versus steam utilization for various operating voltages.

And substituting the above equation in the energy balance yields:

$$SU(V_{op} - V_{tn}) = \frac{C_p}{zF}\Delta T \tag{23}$$

where SU is the steam utilization value, V_{op} is the operating voltage, V_{tn} is the thermoneutral voltage, and ΔT is the change in temperature.

The size of the heat exchanger decreases with the increasing value of steam utilization (lower system mass flows) for all operating voltages. In terms of comparison with the operating voltage, the size of the heat exchanger increases with increasing the voltage up to 1.5 V. Beyond this voltage, the size of the heat exchanger decreases. The variation of the heat exchanger area with steam utilization and operating voltage is given in Figs. 4 and 5.

The efficiency of the electrolysis process reaches maximum at or above the thermoneutral voltage depending on the size of the stack. Efficiency is defined as the energy content of hydrogen divided by the sum of electrical and thermal energy. For a smaller stack the efficiency peaks at around 1.5 V and for a larger stack of around 250 cells, the maximum efficiency is at thermoneutral voltage. Efficiency is not a function of the steam utilization value. The variation of the efficiency of the system with operating voltage is shown in Figs. 6–8 for stack sizes of 10, 50 and 250 cells, respectively. For stack sizes of 10 and 50, the maximum efficiency of 82% is achieved when the operating voltage is greater than the thermoneutral voltage.

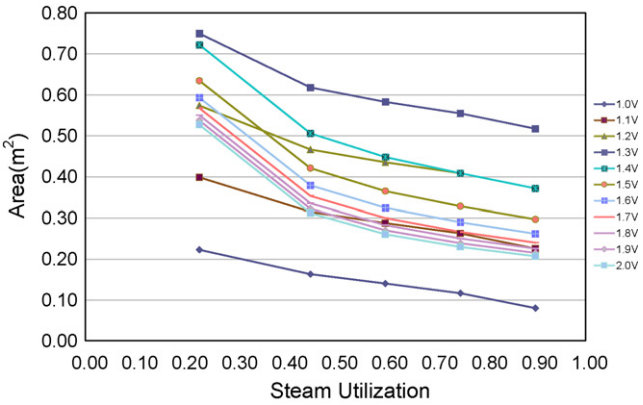

Fig. 5. Area of the heat exchanger versus steam utilization for various operating voltages.

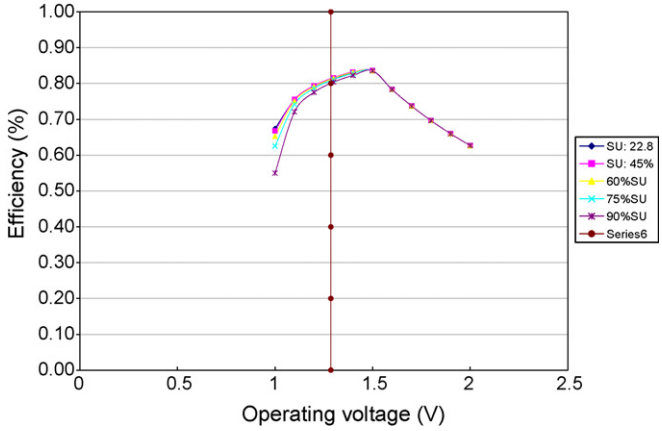

Fig. 6. Efficiency versus steam utilization for various operating voltages for a stack size of 10 cells.

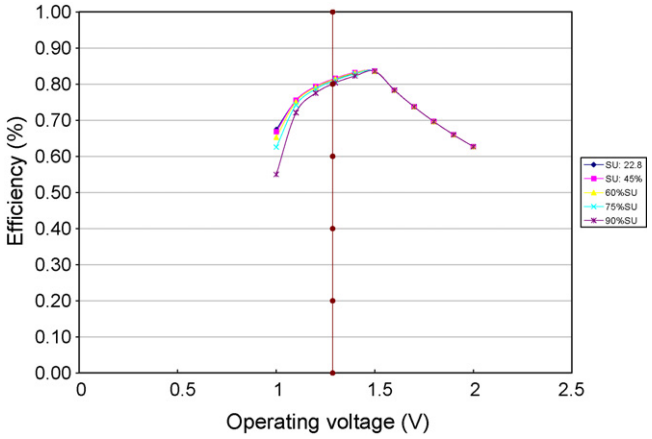

Fig. 7. Efficiency versus steam utilization for various operating voltages for a stack size of 50 cells.

4. Discussion

The temperature of the exiting fuel (steam) and air streams from the SOEC depends on both the operating voltage and the steam utilization value. If the solid oxide electrolysis cell operated at a voltage higher than the thermoneutral voltage the temperature of the gas streams increased with increasing the steam utilization value. If the

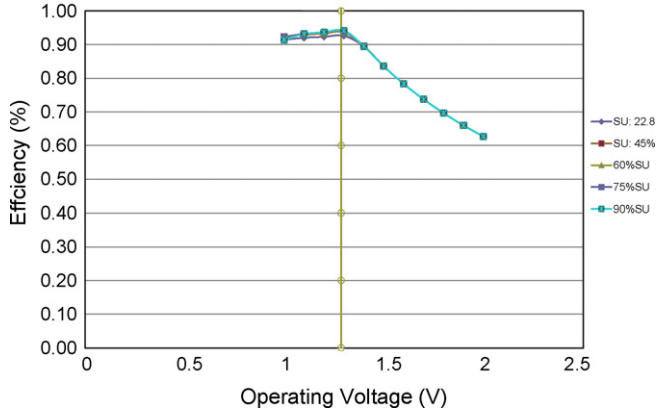

Fig. 8. Efficiency versus steam utilization for various operating voltages for a stack size of 250 cells.

electrolysis cell were operated below the thermoneutral voltage the opposite phenomenon occurred.

The operating voltage also affected the size of the heat exchanger. The size of the heat exchanger increased with the increasing operating voltage up to a maximum, after which it decreased. The point of inflexion was around 1.5–1.6 V. The heat exchanger size decreased with the increase in the steam utilization value but the increase was insignificant above the steam utilization of 0.228.

The efficiency of the electrolysis process increased with the rise in the operating voltage up to a certain voltage beyond which the efficiency is reduced. The tipping point was around 1.5–1.6 V for a stack size of 10 cells. This value started shifting towards the thermoneutral voltage if the number of cells increased significantly. For larger electrolysis cells (with a cell size of 250), the efficiency was constant at about 94% as the voltage increased to the thermoneutral voltage beyond which the efficiency started to decrease. The steam utilization value had an insignificant effect on efficiency.

It is worth noting that a conventional liquid water electrolysis operating voltage is approximately 1.8 V per cell, with advanced cells pushing down the voltage toward 1.6 V per cell. In both conventional water electrolysis and SOEC, hydrogen production is stoichometric with the current. Therefore, in order to have any advantage over conventional electrolysis, the SOEC operating voltage must be less than 1.6 V per cell. Since the thermoneutral voltage is 1.285 V per cell at 1000 K the operating voltage range of interest for thermally self-sustaining SOEC operation is 1.3–1.6 V per cell.

The presented model considered a constant ASR. However, the simulated results showed large variations of temperature in the SOEC system operating at varied operating voltages which in turn can affect the ASR and hydrogen production. More elaborate models may consider the temperature gradient across the system and its effects on the ASR and hydrogen production.

5. Conclusion

We have presented an analysis of heat exchanger and electrolysis cell operation for sources providing both electricity and heat to produce hydrogen. The analysis demonstrates increased efficiency with operating voltages higher than the thermoneutral voltage for a smaller stack size. The higher efficiency for a larger stack size was achieved when the operating voltage was around the thermoneutral voltage. Steam utilization had an insignificant effect on the system efficiency. These results confirm the feasibility of earlier system approaches for using nuclear energy or solar energy to power solid oxide electrolysis cells with higher efficiencies. Additional studies and experiments are needed to confirm the presented analyses and demonstrate efficient operation and cost advantages of the proposed system.

References

[1] L.P.R. Profeti, E.A. Ticianelli, E.M. Assaf, Fuel 87 (2008) 2076–2081.
[2] R.A. Dagle, A. Platon, D.R. Palo, A.K. Datye, J.M. Vohs, Y. Wang, Applied Catalysis A: General 42 (2008) 63–68.
[3] J. Jia, J. Zhou, C. Zhang, Z. Yuan, S. Wang, L. Cao, S. Wang, Applied Catalysis A 341 (2008) 1–7.
[4] J.N. Kuhn, Z. Zhao, A. Senefeld-Naber, L.G. Felix, R.B. Slimane, C.W. Choi, U.S. Ozkan, Applied Catalysis A 341 (2008) 43–49.
[5] A. Perna, International Journal of Hydrogen Energy 33 (2008) 2957–2964.
[6] X. Vitart, A. Le Duigou, P. Carles, Energy Conversion and Management 47 (2006) 2740–2747.
[7] N.H. Florin, A.T. Harris, International Journal of Hydrogen Energy 32 (2007) 4119–4134.
[8] S. Licht, International Journal of Hydrogen Energy 30 (2005) 459–470.
[9] S. Licht, Electrochemistry Communications 4 (2002) 790–795.
[10] S.S. Kocha, D. Montgomery, M.W. Peterson, J.A. Turner, Solar Energy Materials and Solar Cells 52 (1998) 389–397.
[11] V.M. Aroutiounian, V.M. Arakelyan, G.E. Shahnazaryan, G.M. Stepanyan, J.A. Turner, O. Khaselev, International Journal of Hydrogen Energy 27 (2002)33–38.
[12] S. Licht, B. Wang, S. Mukerji, T. Sogab, M. Umenob, H. Tributsch, International Journal of Hydrogen Energy 26 (2001) 653–659.
[13] S. Licht, Solar Energy Materials and Solar Cells 38 (1995) 305–319.
[14] S. Licht, S. Ghosh, H. Tributsch, S. Fiechter, Solar Energy Materials a Solar Cells 70 (2002) 471–480.
[15] J.R. Thompson, R.D. McConnell, M. Mosleh, Cost analysis of a concentrator photovoltaic hydrogen production system, in: International Conference on Solar Concentrators for the Generation of Electricity or Hydrogen (NREL/CD-520-38172), 1-5 May 2005, Scottsdale, Arizona, 2005.
[16] S. Fujiwara, S. Kasai, H. Yamauchi, K. Yamada, S. Makino, K. Matsunaga, M. Yoshino, T. Kameda, T. Ogawa, S. Momma, E. Hoashi, Progress in Nuclear Energy 50 (2008) 422–426.
[17] S. Herring, J.O. Brien, C.M. Stoots, G.L. Hawkes, J. Hartvigsen, M. Shahnam, International Journal of Hydrogen Energy 32 (2007) 440–450.
[18] J.O. Brien, C.M. Stoots, S. Herring, J. Hartvigsen, 158 (2007) 118–131.
[19] S. Herring, J.O. Brien, C.M. Stoots, G.L. Hawkes, J. Hartvigsen, High temperature electrolysis for hydrogen production using nuclear energy, Proceedings of Global 2005, Tsukuba, Japan, October 9–13, 2005, Paper No. 501.
[20] M. Ni, M.K.H. Leung, D.Y.C. Leung, International Journal of Hydrogen Energy 33 (2008) 2337–2354.
[21] R.K. Shah, International Journal of Heat Mass Transfer 18 (1975) 849–862.
[22] M. Liu, B. Yu, J. Xu, J. Chen, Journal of Power Sources 177 (2008) 493–499.
[23] F.C.C. Galeazzo, R.Y. Miura, J.A.W. Gut, C.C. Tadini, Chemical Engineering Science 61 (2006) 7133–7138.